Case Studies in Construction Materials 19 (2023) e02573

Contents lists available at ScienceDirect

Case Studies in Construction Materials

journal homepage: www.elsevier.com/locate/cscm

Rheological and mechanical consequences of reducing the curing time of cold asphalt mixtures by means of magnetic induction

Christopher DeLaFuente-Navarro [a,c], Pedro Lastra-González [a], Miguel Ángel Calzada-Pérez [b], Daniel Castro-Fresno [a,*]

[a] GITECO Research Group, Universidad de Cantabria, Avda. de Los Castros s/n., 39005 Santander, Spain
[b] GCS Research Group, Universidad de Cantabria, Avda. de Los Castros s/n., 39005 Santander, Spain
[c] School of Civil Construction, Faculty of Engineering, Pontificia Universidad Católica de Chile, Avenida Vicuña Mackenna 4860, Santiago, Chile

ARTICLE INFO

Keywords:
Porous asphalt
Cold asphalt mixture
Magnetic induction
Virgin steel fiber
Curing time
Rheological properties

ABSTRACT

Cold asphalt mixtures are more sustainable because they are manufactured at ambient temperature. However, they are much less applied because they take longer time in the curing process due to the water contained in the asphalt emulsion, which delays the opening of roads. To solve this problem, the option of adding magnetic aggregates to cold asphalt mixtures and heating them by magnetic induction to evaporate the water contained in the asphalt emulsion and reduce curing time has been evaluated. For this objective, different by-products were evaluated as magnetic aggregate and the best one was selected. Four porous asphalt mixtures were then manufactured: an experimental mixture with the selected magnetic particles, a control mixture with virgin steel instead of the by-products, and two oven-cured reference mixtures without magnetic aggregate (one according to the Spanish standard and another according to the U.S. Asphalt Institute guidelines); then, the four mixtures were studied in terms of the curing process, rheological properties of bitumen and mechanical performance of samples. The experimental mixture containing industrial by-products shortened the curing time from 7 and 2 days (Spanish and U.S. Asphalt Institute standard, respectively) to only two hours; rheological and mechanical analysis proved the viability of this technology.

1. Introduction

Cold asphalt mixtures consume less energy and generate lower greenhouse gas emissions than their hot asphalt counterparts [1–3]. In particular, producing one ton of cold asphalt mixture requires 5% of the energy required to produce the same amount of hot asphalt mixtures [4]. Similarly, the production of one ton of cold mixture leads to 40% reduction in greenhouse gas emissions [5].

However, cold asphalt mixtures require time to reach their maximum resistance [1,8,9] mainly by the water evaporation of the bituminous emulsion [6,7]. For this reason, cold asphalt mixtures have been set aside. For example, between 2015 and 2017, 44,700, 000 tons of hot mixtures were executed in Spain compared to 364,000 tons of cold mixtures [10].

For the above reason, reducing the duration of the curing process of cold asphalt mixtures would favor the use of a mix that involves lower energy consumption, lower greenhouse gas emissions and greater safety by not executing the works at high temperatures. In this

* Corresponding author.
E-mail addresses: Christopher.delafuente@unican.es (C. DeLaFuente-Navarro), Pedro.lastragonzalez@unican.es (P. Lastra-González), Miguel.calzada@unican.es (M.Á. Calzada-Pérez), Castrod@unican.es (D. Castro-Fresno).

https://doi.org/10.1016/j.cscm.2023.e02573
Received 21 August 2023; Received in revised form 10 October 2023; Accepted 12 October 2023
Available online 13 October 2023

regard, there are only two researches related to this novel process: Perez [11] and Lastra-Gonzalez [12] addressed this issue using magnetic induction; however, their studies did not delve into the consequences of the magnetic induction in the rheological and mechanical properties of the pavement. In addition, [11] and [12] studied asphalt mixtures with virgin steel fiber as magnetic aggregate, which significantly increases costs and carbon dioxide emissions [13,14].

Because of the above, the objective of this research was to evaluate at laboratory level a new process of fast curing of cold asphalt mixtures with respect to the traditional method. Additionally, the feasibility of replacing the virgin steel usually applied to cure asphalt mixtures by magnetic by-product was also assessed. Furthermore, to determine the rheological implications on the bitumen and the mechanical consequences on the mixture of this new curing process in order to assess its feasibility.

For this purpose, four different porous mixtures were manufactured:

- Two reference mixtures without magnetic particles cured in an oven, one according to the Spanish standard [15] and the second according to the guidelines of the U.S. Asphalt Institute [16].
- Two experimental mixtures with magnetic aggregates cured by magnetic induction: one manufactured with virgin steel fibers and another experimental asphalt mixture with the best industrial by-product among the analysed.

The four cold asphalt samples were compared in terms of their curing process, rheological properties of the bitumen and mechanical properties of the mixtures. The results were evaluated by statistical analysis using Minitab software.

2. Materials

A commercial cationic emulsion C60BP4 MIC was used as binder. It is commonly applied in cold microagglomerates and contains 40% water and 60% of polymer-modified bitumen with a medium breaking time. Its characteristics are summarized in Table 1.

The aggregates considered for the design of the cold asphalt mixtures are ophite as coarse fraction and limestone as fine and filler fraction; their characteristics are summarized in Table 2.

Five by-products were magnetically evaluated to select the best one, which was later included in the experimental asphalt mixture.

The five by-products correspond to green foundry slag, steel shavings, fibers residues, steel powder and steel shot blasting. Fig. 1 shows them together with the virgin steel fibers.

The magnetic aggregates were characterized by calculating their density and particle size distribution, summarized in Table 3.

3. Methodology

The research was divided into four phases. First, before manufacturing the mixtures, the by-products were analyzed with respect to their magnetic susceptibility in order to select the most suitable one. In the second phase of the research, the curing process of the reference and experimental mixtures was compared with respect to curing time, energy consumption and water evaporated. Then, in the third phase, the rheological consequences of the different curing methods on the bitumen were evaluated. Finally, in the fourth phase, the mechanical properties of the four mixtures were evaluated to assess the feasibility of the process.

3.1. Phase 1: evaluation and selection of the magnetic by-products to manufacture the experimental mixtures

In order to select the most suitable by-product for the experimental mixture, the thermal homogeneity, heat capacity and the rate at which the magnetic aggregate lost temperature were evaluated.

In this task, the same induction protocol was applied to every metallic particle: the intensity was 400 A for 120 s and 180 s cooling time. The thermal response of each sample was recorded in real time by using an Optris PI Connect infrared thermal camera. The same coil was used, the volume of material was always the same and the distance from the surface of the samples to the coil was constant (2 cm), since the magnetic field decreases as the coil is moved away from the material [17–19] [20,21].

Then, the heating and cooling rate of each by-product was calculated to know the magnetic sensitivity and temperature loss. These rates were obtained using the following Eq. 1:

$$Heating \quad or \quad cooling \quad rate = \frac{\Delta Temperature}{Time} \tag{1}$$

The thermal homogeneity of the by-products was obtained by comparing the average temperature of the sample with the hottest point.

3.2. Phase 2: evaluation between oven curing process and magnetic induction curing process of cold asphalt mixtures

In this phase, to evaluate and compare the four curing processes, the amount of evaporated water was determined: the samples were weighed before and after the curing process. At the same time, the energy consumed by the equipment involved in each curing process was determined: the total kW was calculated.

To achieve the objective of this phase, four cold porous asphalt mixtures were manufactured with a high percentage of voids to facilitate potential water evaporation: the first according to the Spanish standard (Ref. Spain) [15], the second according to the guidelines of the U.S. Asphalt Institute (Ref. U.S.) [16], the third cured by magnetic induction with virgin steel particles (EM1) and the

Table 1
Emulsion properties.

Emulsion properties	Value	Stantard
Polarity	Positive	-
Breakage value (g)	180	EN 13075–1
Residual binder content (%)	61	EN 1428
Creep time (2 mm, 40°C)	45	EN 12846–1
Settling tendency (7 days)	7.5	EN 12847
Sifting residue (0.5 mm)	0.03	EN 1429
Penetration (mm, 25°C)	80	EN 1426
Softening point (°C)	50	EN 1427

Table 2
Properties of aggregate.

Aggregate	Property	Value	Limit	Standard
Ophite	Los Angeles coefficient (%)	13	≤ 20	EN 1097–2
	Specific weight (g/cm3)	2.787	-	EN 1097–6
	Polished stone value (PSV)	60	≥ 56	EN 1097–8
	Flakiness Index (%)	8	≤ 20	EN 933–3
Limestone	Los Angeles coefficient (%)	24	-	EN 1097–2
	Specific weight (g/cm3)	2.705	-	EN 1097–6
	Sand equivalent (%)	78	> 55	EN 933–8

Fig. 1. Magnetic aggregates.

Table 3
Properties of potential magnetic aggregates.

Aggregate	Density	Sieve (%)						
	g/cm^3	8	4	2	1	0.5	0.25	0.063
Green foundry slag	7.288	100	100	100	97	52	19	6
Steel shavings	7.639	-	-	-	-	-	-	-
Fiber residue	3.580	100	100	100	100	82	47	0
Steel powder	8.044	100	100	100	100	100	88	26
Steel shot blasting	7.435	100	100	100	100	67	14	0
Virgin steel fibers	7.800	100	100	100	100	0	0	0

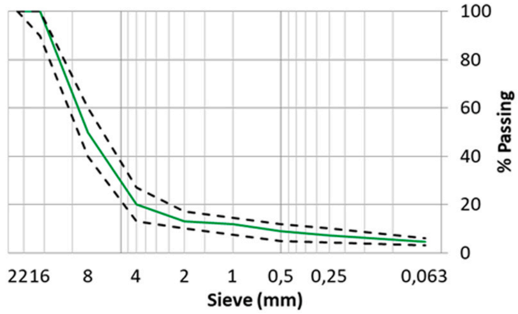

Fig. 2. Particle size distribution of all the samples studied in this research.

fourth cured by magnetic induction with the by-product selected in the previous phase (EM2).

All reference and experimental mixtures had the same particle size distribution in order to evaluate them under equal conditions, as shown in Fig. 2.

The binder content directly affects the magnetic capacity of the mixture [22]. In this case, the percentage of bitumen of the four mixtures studied was 4.5% by weight of mixture.

The first reference mixture (Ref. Spain) was cured according to the Spanish standard [15]: it was introduced in an oven at 75 ± 2 °C for 48 h. Then, at the end of this period, it was verified that there was not drainage of binder at the base of the samples. Then, the temperature was increased to 90 ± 2 °C for five more days. At the same time, with respect to the second reference mixture (Ref. U.S.), this was cured according to the U.S. Asphalt Institute standard [16]: it was placed in an oven at a temperature of 60ºC for 48 h, what means there are 5 days of difference between both standards.

Regarding the manufacture of experimental mixtures, both were added 1% magnetic particles with respect to the volumen of the mixture (2% of magnetic material by with weight of the mixture). It is very important to avoid the formation of magnetic particle clusters and to achieve a homogeneous temperature in order to ensure a good performance of the final mixtures and thus avoid specific points with very high temperatures [23]. Unfortunately, manufacturing cold asphalt mixtures cured by induction heating is a very innovative process without a standard protocol. For this reason, the magnetic particles were added after the emulsion together with the filler; therefore, the conventional aggregates are coated first by the emulsion. The experimental mixtures were also compacted applying 50 blows per face with the Marshall hammer.

In this case, regarding the curing process of the experimental mixtures, a magnetic induction protocol was designed for each type of magnetic aggregate. The objective of the protocol was to get rid of the water after taking the mixture to a temperature of 100ºC so that this reduced as far as possible the curing time [24].

Magnetic induction was applied for 25 min to cure both experimental mixtures; then, they were allowed to cool for 95 min at ambient temperature. Table 4 shows these protocols for EM1 (virgin steel) and EM2 (by-product).

The EM1 mixture was cured applying lower energy because the virgin steel fibers had higher magnetic sensitivity, this magnetic particle is made of pure steel and has a larger particle size.

The average and maximum temperature were controlled by an infrared camera located above the surface of the specimens. The magnetic field was applied by a Easyheat LI 3542 high-frequency induction machine. A helical coil was used to achieve homogeneous heating, so that the controlled temperature at the top is equal to the one at the bottom. The distance from the coil to the sample was always the same, since this is closely related to the heating rate of the sample [23]. Fig. 3 presents the condition of the induction process.

3.3. Phase 3: evaluation of the impact of the curing process on the rheological properties of bitumen

Due to the fact that each curing method involves a different thermal process, their impact on the rheological properties of the bitumen was studied [25]. For this purpose, the bitumen was recovered by the rotary evaporator process, as described in the UNE-EN 12697–3 standard. Then, the penetration degree is determined by needle at 25 °C (EN 1426), the softening point from 5ºC by ring and ball test (EN 1427), and viscosity, stiffness and phase angle by dynamic shear rheometer (DSR) test. The temperature range studied was

Table 4
Curing protocols.

Mixture	Steps	Intensity (A)	Power (W)	Time (minutes)
EM 1	1	290	2565	1
	2	80	160	4
	3	50	19	20
EM 2	1	290	1455	10
	2	330	1463	3
	3	400	1474	8
	4	450	1505	4

Fig. 3. Magnetic induction equipment.

from 60 °C to 20 °C with measurement every 5 °C and the frequency in oscillatory mode was from 0.1 Hz to 30 Hz (EN 14770). Fig. 4 shows the configuration of the tests carried out in this phase.

Then, with the data obtained in DSR, the master stiffness curve of the four bitumens was determined to analyze the rheological characteristics of the binder independently from frequency and temperature. To obtain the master curve, the stiffness results were fitted to a sigmoidal least-squares curve [26,27] according to Eq. 2.

$$\log(|G^*|) = \alpha + \frac{\beta}{1 + e^{\gamma - \mu \log(f_r)}}(MPa) \tag{2}$$

Where α is lower asymptote, β is the variance between the asymptotes upper and lower values, γ and μ are shape parameters, f_r is the reduced frequency (f_r relates the f frequencies of the test to temperatures A_t) according to Eq. 3.

$$f_r = A_t \quad \bullet f \quad \left(\frac{rad}{s}\right) \tag{3}$$

A_t is defined according to Eq. 4.

$$\log(A_t) = A_1 T^2 + A_2 T + A_3 \tag{4}$$

Where T is the temperature in degrees Celsius and $A_1, A_2 and \quad A_3$ are shape parameters.

3.4. Phase 4: mechanical evaluation of the cold asphalt mixtures

The feasibility of the magnetic induction method was evaluated by assessing the mechanical performance of the reference and experimental mixtures. Different tests were applied to evaluate the four cold asphalt mixtures performance: the internal structure of the specimens was calculated by the voids test (EN 12697–8). The cohesion of the mixtures was evaluated by the Cantabro particle loss test at 25 °C (EN 12697–17). The stiffness of the specimens was calculated by applying a strain of 50 µm per pulse at 20 °C (EN12697–26), and the indirect tensile strength (I.T.S.) was determined at 15 °C by breaking the specimens at a rate of 5 mm per second (EN12697–23). The temperature of all samples was controlled to avoid variations in performance [28]. The configuration of the three mechanical tests carried out is shown in Fig. 5.

All tests were performed by testing at least 4 specimens and 48 h elapsed from the end of the curing process of the specimens before they were subjected to mechanical tests.

Once the results of the tests were obtained, a statistical evaluation was performed using Minitab software with 95% confidence interval to determine if there was a significant difference between the results obtained. If the results turned out to be parametric; that is, they had a normal distribution and homogeneity of variance, t-Student was applied. Otherwise, U-mann Whitney was used for non-parametric results. The experimental mixture with by-product (EM2) was compared with the two reference mixtures (Ref. Spain and Ref. U.S. institute) and with the mixture with virgin steel (EM1).

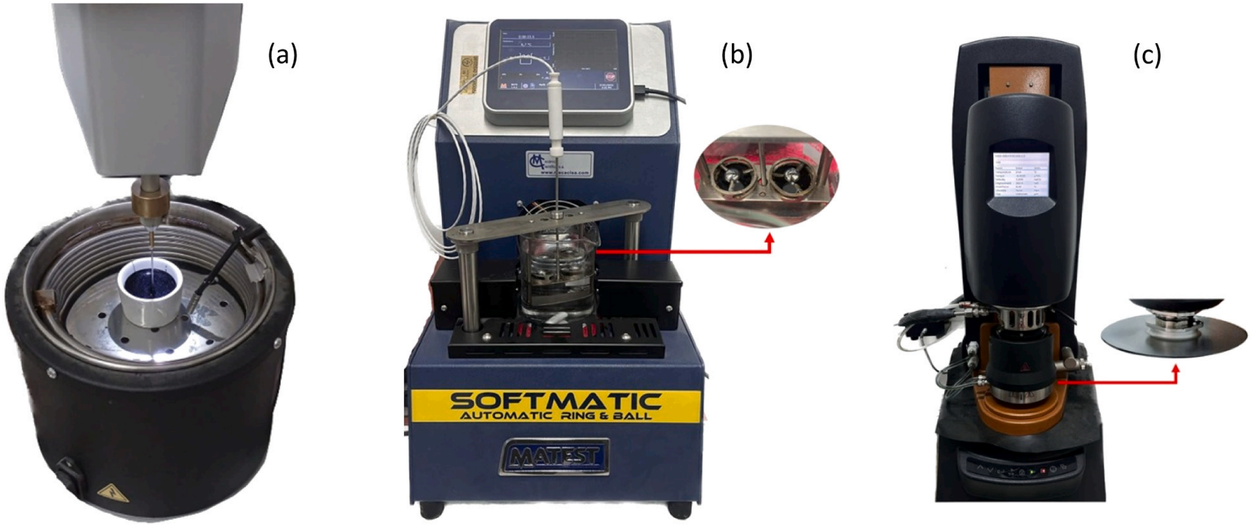

Fig. 4. Rheological test of the binder. (a) Penetration test. (b) Ring and ball test. (c) Dynamic shear rheometer.

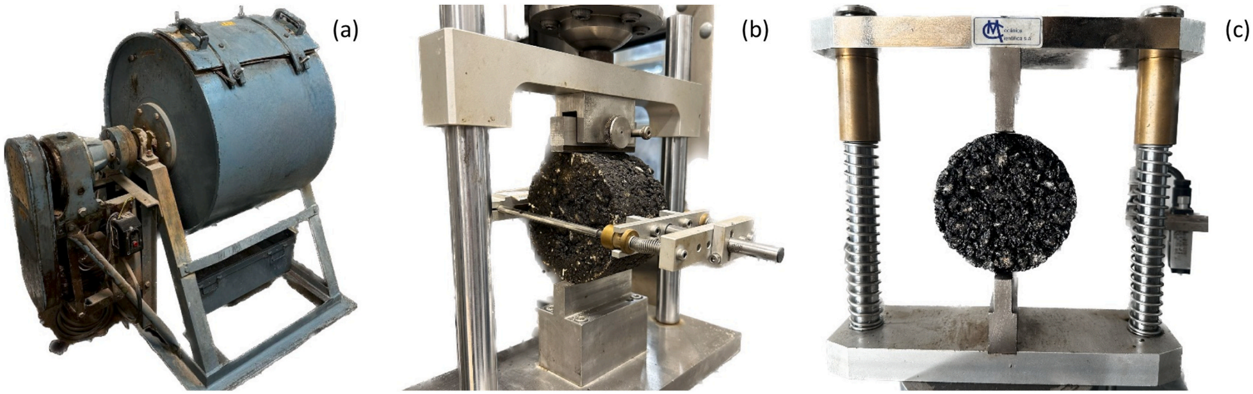

Fig. 5. Mechanical tests. (a) Angeles machine for Cantabro test. (b) Stiffness test. (c) Indirect tensile strength test.

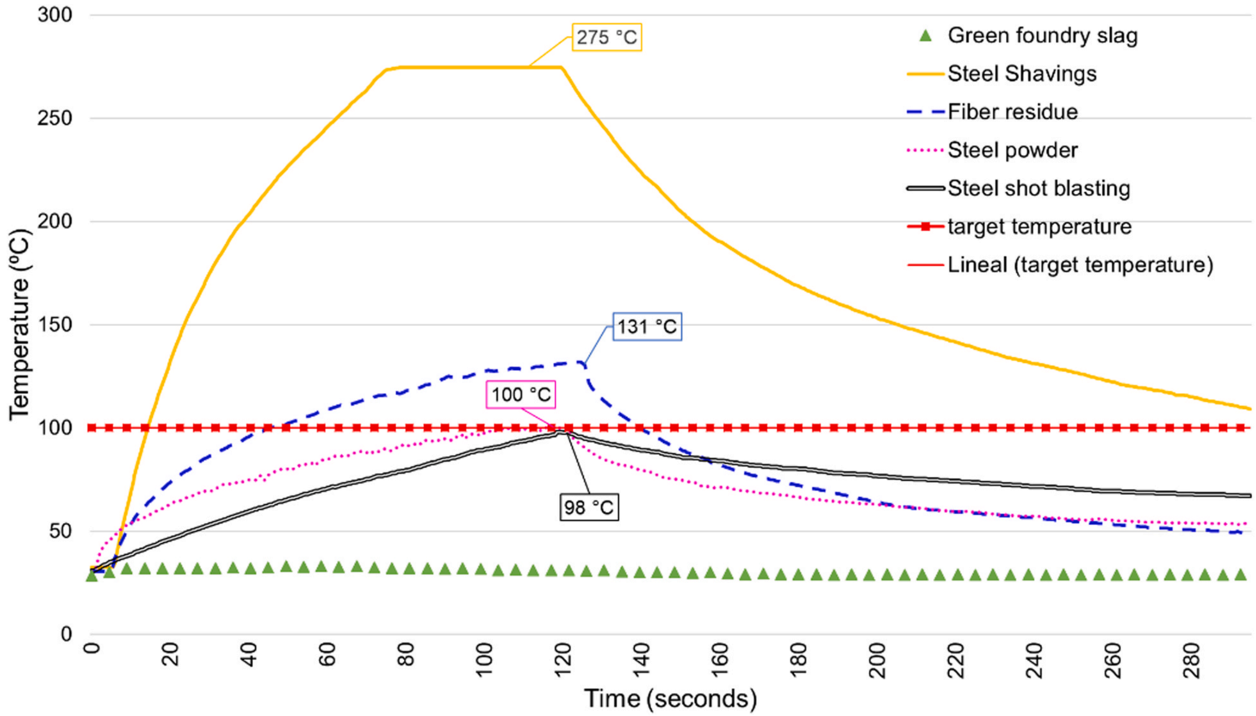

Fig. 6. Temperatures obtained from the Magnetic Induction test on by-products.

Table 5
Rates of temperature rise and loss during magnetic field exposure and cooling cycle.

Temperature gain in relation to time.				
Green foundry slag	Steel shavings	Fiber residue	Steel powder	Steel shot blasting
0.02 °C/s	2.01 °C/s	0.84 °C/s	0.61 °C/s	0.56 °C/s
Energy loss in relation to time				
Green foundry slag	Steel shavings	Fiber residue	Steel powder	Steel shot blasting
-0.02 °C/s	-1.74 °C/s	-0.98 °C/s	-0.61 °C/s	-0.29 °C/s
Rate differential: gain vs. loss of temperature				
0.00 °C/s	0.27 °C/s	-0.14 °C/s	0.00 °C/s	0.27 °C/s

4. Results and discussion

4.1. Phase 1 results: evaluation and selection of the magnetic by-product to manufacture the experimental mixture

The results obtained from the magnetic induction test on by-products are shown in Fig. 6.

With regard to Fig. 6, while the lowest susceptibility was reached by green foundry slag whose temperature did not vary, it was discarded from the study.

In the case of steel powder, steel shot blasting and fiber residues, the magnetic susceptibility was similar. Table 5 presents the magnetic susceptibility with the growth and decrease rates.

Steel shot blasting and steel shavings showed the best temperature equilibrium; both ended the process with a positive differential rate of 0.27 °C/s, which means that they gained more temperature in the heating-cooling process. This point is important because these two materials potentially increase the water evaporation rate during the cooling process after applying magnetic induction. Then, in comparison, the fiber residue and the steel powder both showed a lower heating-cooling ratio; as a result, they were discarded.

Regarding the choice between the steel shavings and the steel shot blasting, the first was discarded because they presented some practical problems: their thermal susceptibility was not homogeneous and their shape made its homogeneous distribution in the mixtures very difficult (Fig. 7). Therefore, the steel shot blasting was selected as the best by-product.

4.2. Phase 2 results: evaluation of the curing process

The results of each curing protocol, having measured the amount of water in the samples before and after the process, are summarized in Table 6.

With respect to Table 6, magnetic induction technology appears as a useful procedure to improve the performance of the curing process, since it manages to evaporate the same amount of water reducing considerably the time spent. Furthermore, virgin steel fibers and steel shot blasting did not mean a time variation in relation to the curing process among the specimens subjected to magnetic induction. Fig. 8 presents the different cured mixtures; no visual differences were observed.

Then, Fig. 9 below shows the amount of energy consumed by the equipment in each curing process.

The two experimental samples required very little curing energy compared to the two reference mixtures, what can be explained by the fact that the magnetic induction technology heats only the magnetic particles with a high thermal capacity, whereas the reference oven-curing method must heat the entire mixture.

Therefore, the application of magnetic induction allows for a significant reduction in curing energy and time compared to reference oven curing methods. For the above mentioned, the study of rheological and mechanical properties will validate the feasibility of this technology.

Fig. 7. Left, shavings of steel particles; right, shavings of steel debris after magnetic induction process.

Table 6
Consolidation of results of the curing protocols.

Mixture	Curing protocol	Time of curing	Water evaporated (%)
Ref. Spain	Cured by oven	7 days	95 ± 4
Ref. U.S.	Cured by oven	2 days	93 ± 6
EM1	Curing protocol 1	2 h	95 ± 3
EM2	Curing protocol 2	2 h	94 ± 3

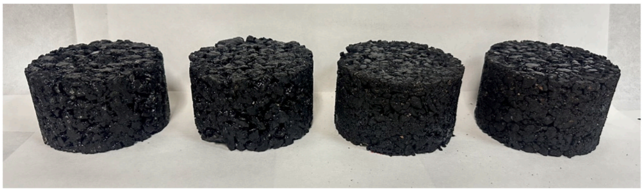

Fig. 8. Example of the different mixtures. From left to right: Ref Spain, Ref U.S. Institute, EM1 and EM2.

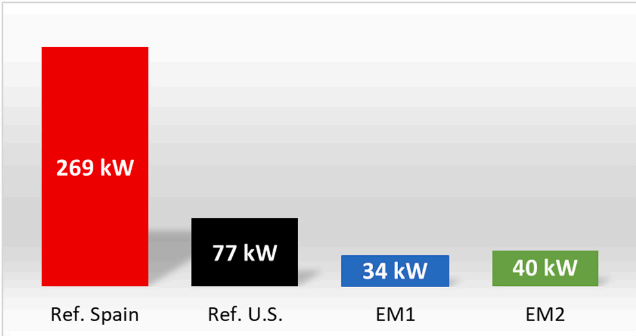

Fig. 9. Curing energy of each curing process.

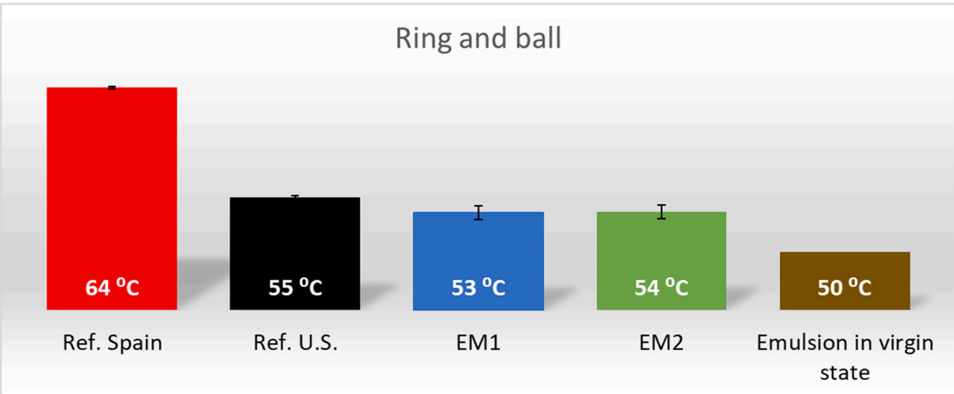

Fig. 10. Ring and ball test results.

4.3. Phase 3 results: evaluation of the impact of the curing process on the rheological properties of bitumen

As described in the methodology, the rheological properties of the bitumen were evaluated to determine the consequences of magnetic induction curing on the bitumen. Initially, Fig. 10 and *Fig.* 11 show the results of the ring and ball and penetration tests.

Respect to Fig. 10 and Fig. 11, Ref. Spain had a higher softening point and lower penetration than Ref. U.S. and at the same time, Ref. U.S. had a slightly higher softening point and slightly lower penetration than EM1 and EM2. This means that the shortening of the curing time by applying magnetic induction decreases the short-term aging, which implies a more flexible and soft binder.

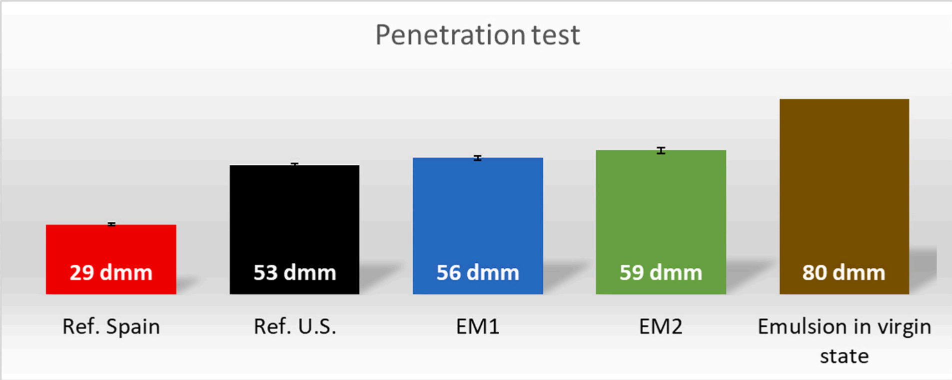

Fig. 11. Penetration test results.

Regarding the DSR test, Fig. 12 shows that Ref. Spain has a higher viscosity, which can be explained by the long time it remains at a high temperature during its curing process. At the same time, as in the penetration and ring and ball tests, the Ref. U.S. bitumen has a slightly higher viscosity than the two experimental samples. This result supports the theory that shortened curing time allows for less short-term aging.

With respect to Fig. 13, it is possible to visualize that Ref. Spain bitumen is notoriously stiffer than the rest of the samples, followed by Ref. U.S. and then by the two experimental samples. The stiffness exhibited in each of the bitumens agrees with the viscosity grade evaluated in Fig. 12.

At the same time, in Fig. 14, the lowest phase angle was obtained by Ref. Spain, so it has a lower capacity to store and dissipate energy during deformation. Similarly to the previous evaluations, Ref. U.S. had a slightly lower phase angle than the bitumens in the experimental mixtures. Therefore, the stiffness and phase angle results match the performance of the bitumens in the penetration, ring and ball and viscosity evaluations.

Then, master curves were developed for each bitumen. In Fig. 15, it can be seen that Ref. Spain has a higher complex modulus for all reduced frequencies(f_r). and is followed by Ref. U.S., which is again very similar to that of the bitumen in the experimental mixtures. This means that, irrespective of frequency and temperature, the behavior of bitumen Ref. Spain will have a higher stiffness.

The rheological analysis of bitumens recovered from the four mixtures studied in this investigation showed that the curing method used for Ref. Spain increases the short aging of the bitumen (higher stiffness, lower capacity to store and disperse energy, higher hardness and a higher softening point). At the same time, the bitumen extracted from Ref. U.S. is slightly more aged than the bitumen recovered from the experimental mixtures. However, there were not differences between both experimental mixtures. These results will directly affect the mechanical performance of the asphalt mixtures.

4.4. Phase 4 results: mechanical evaluation of the cold asphalt mixtures

The mechanical behaviour to ensure the performance of the experimental cold asphalt mixtures was studied. Initially, the mixtures were characterized by calculating the percentage of voids (EN 12697–8). The results are summarized in Table 7.

The difference in the percentage of voids is not significant, so it cannot be considered a determining factor in the mechanical performance of the mixtures.

The results of the Cantabro particle loss are presented in Fig. 16 and Fig. 17.

The experimental mixtures cured by induction heating decreased significantly their particle loss. Although there are no statistical differences between both experimental mixtures, there is a statistically significant difference between the two experimental mixtures and the two reference mixtures (p-values are presented in Table 8). As the percentage of voids is almost the same, any influence of the internal structure is ruled out. Despite the possible influence of the magnetic particles, the conclusion of the rheological study on the low level of binder aging of the experimental mixtures is considered to be the most likely reason for this significant improvement of the experimental mixtures.

Secondly, the results of modulus of stiffness and I.T.S. are presented in Fig. 18 and Fig. 19.

Respect to Fig. 18 and Fig. 19, the theory that the magnetic induction decreases the aging of the residual bitumen is consistent with the results of the I.T.S. and stifness. Meanwhile, in both tests, the Ref. Spain, which is the mixture with more time in oven, presented the highest resistance. The Ref. U.S. is in an intermediate position, while the experimental mixtures have the lowest resistances being statistically significant. Among the experimental mixtures the results were very similar (p-values are presented in Table 8).

Taking into account that the particle size distribution and the type of aggreages are the same for all mixtures, this point is coherent with the fact the binder of the mixtures cured by induction is lower aged than the residual bitumen of the mixtures cured by oven.

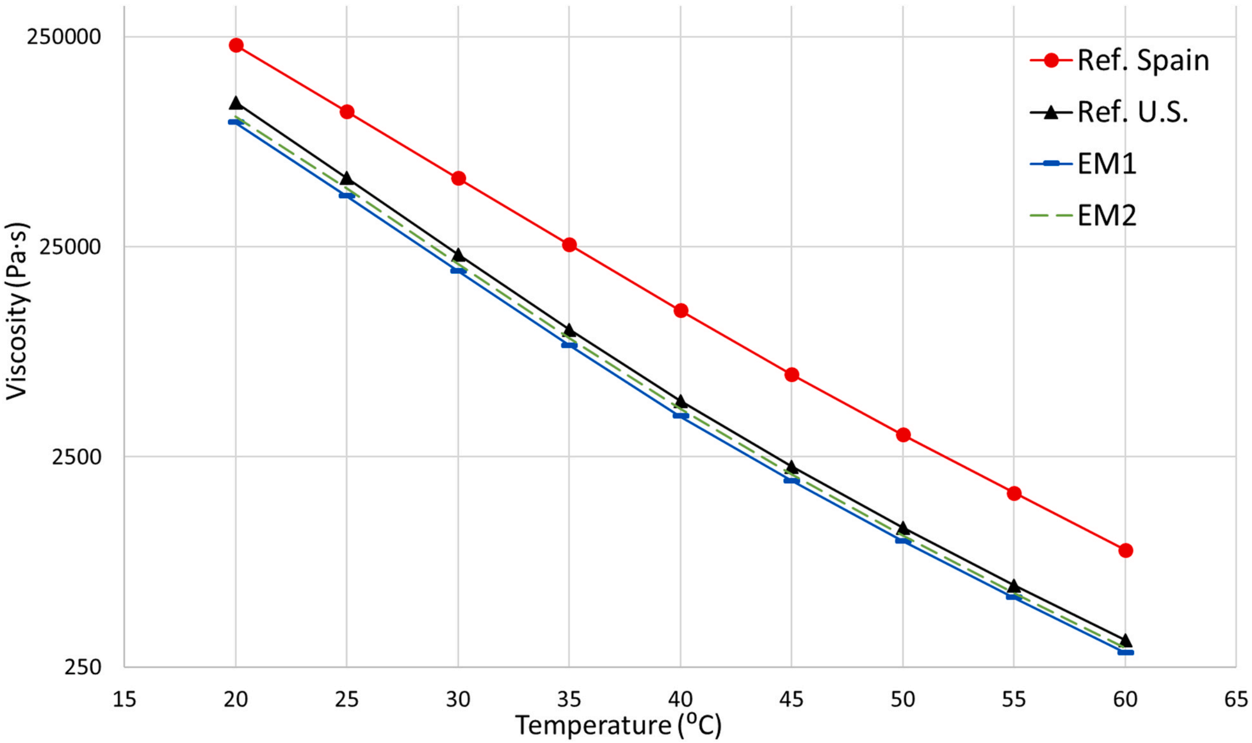

Fig. 12. Result of the viscosity test.

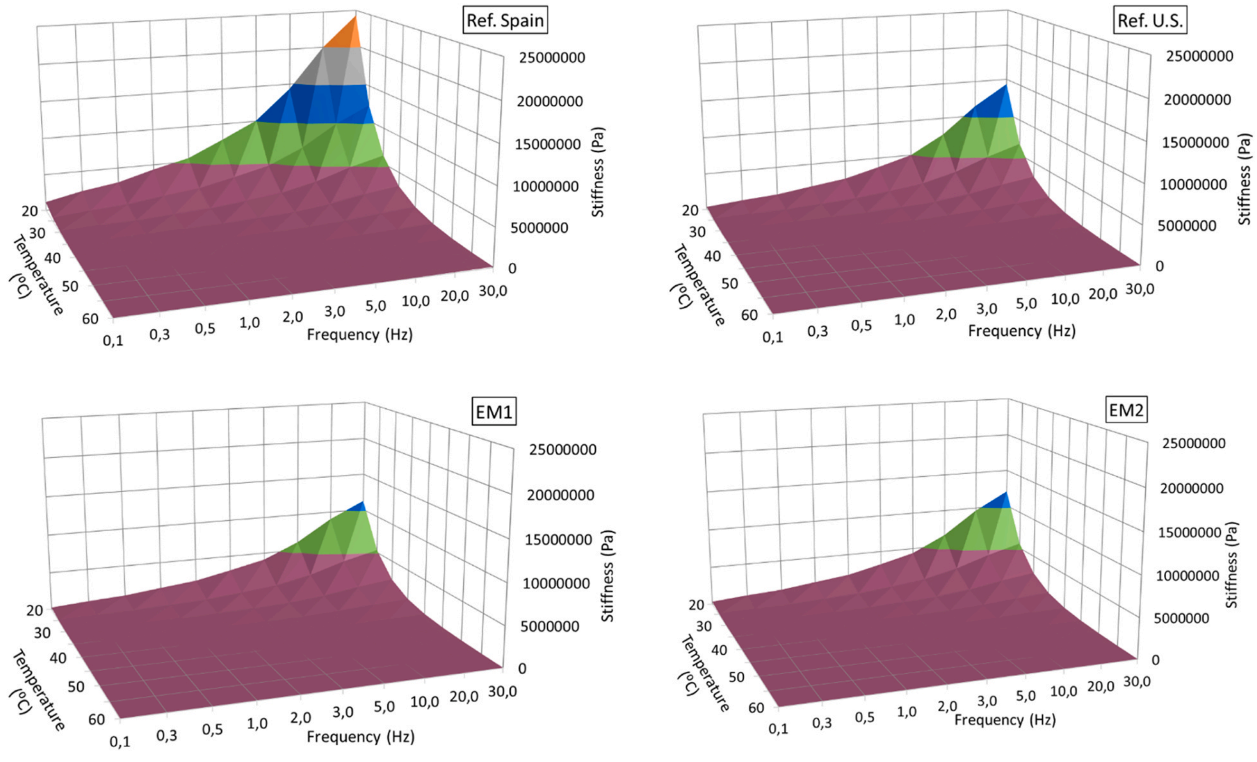

Fig. 13. Result of the Stiffness of bitumen in DSR.

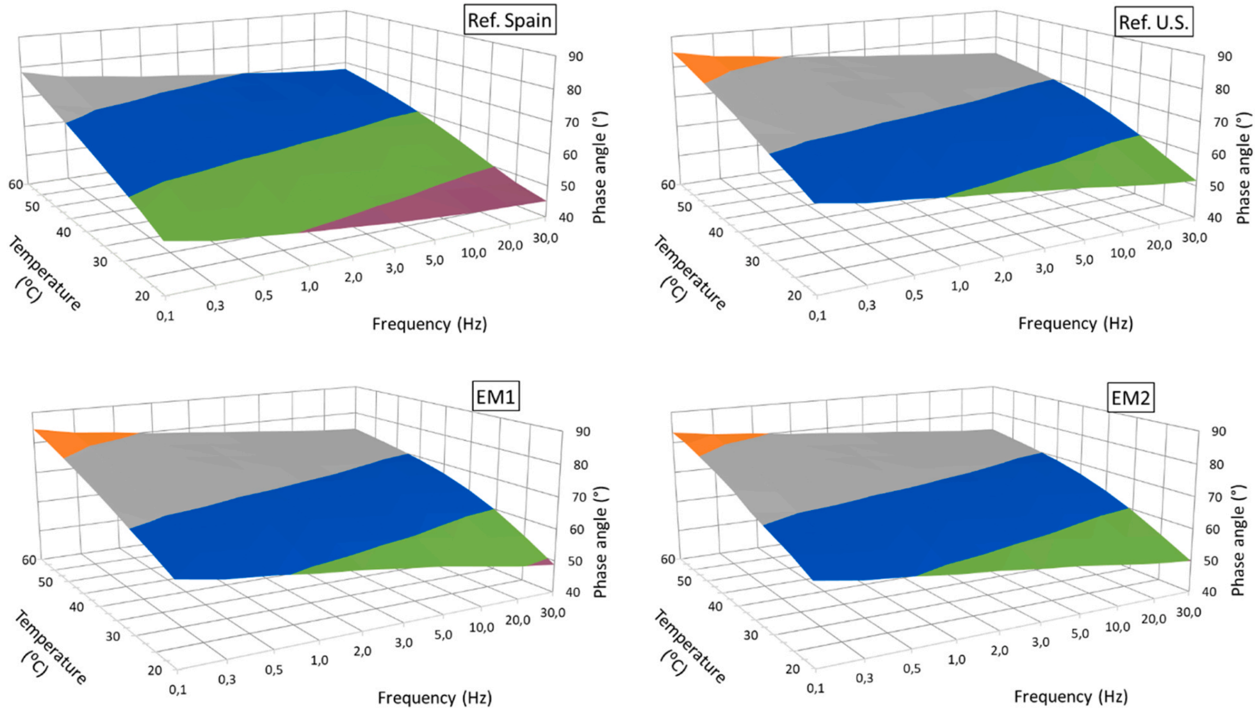

Fig. 14. Result of phase angle of bitumen in SDR.

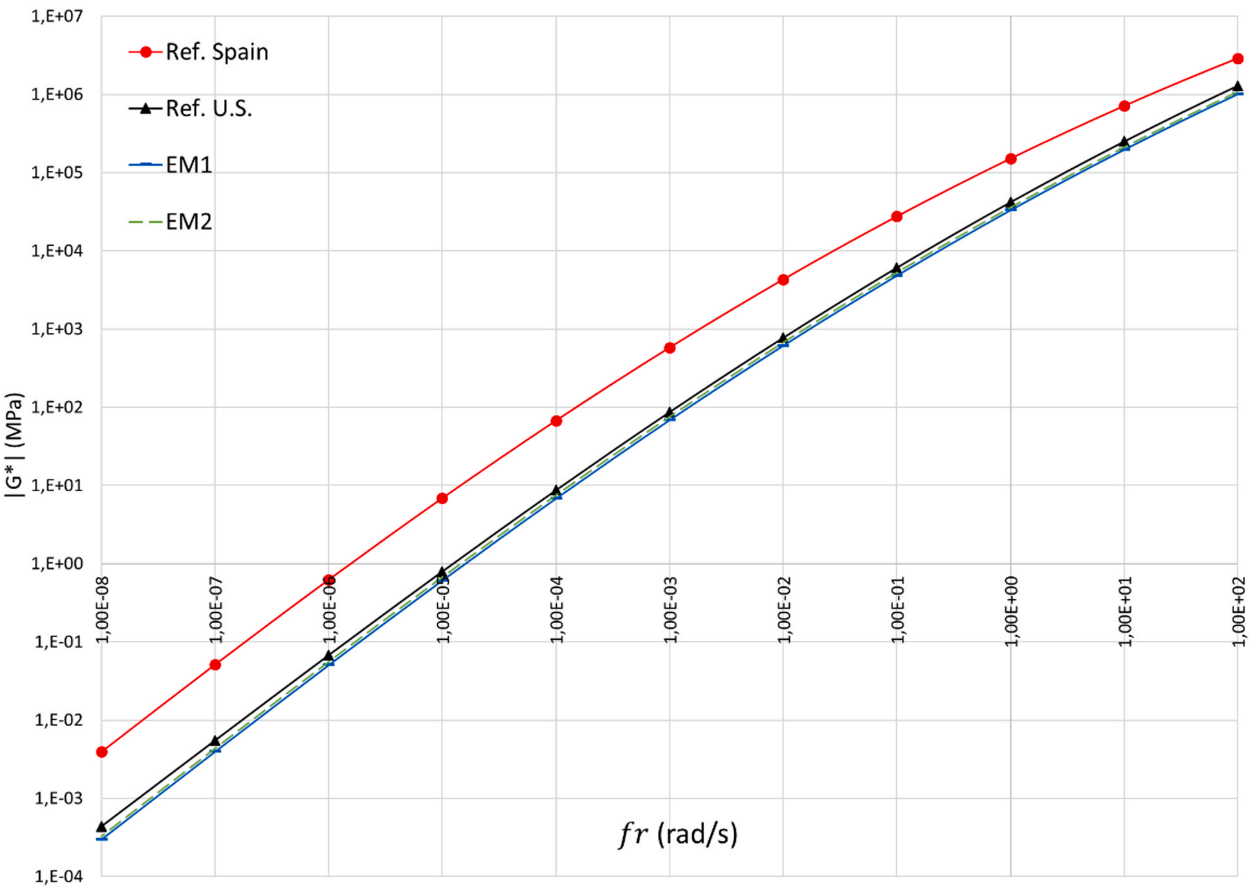

Fig. 15. Master curves of bitumen.

Table 7
Void measurement results.

Mixture	Magnetic material	Density (g/cm^3)	Voids (%)
Ref. Spain	-	2.777	25.4 ± 0.7
Ref. U.S.	-	2.777	25.0 ± 0.4
EM1	virgin steel	2.810	25.3 ± 0.4
EM2	by-product	2.824	25.7 ± 1.1

Fig. 16. Final condition of samples sometimes tested in Cantabro. From left to right: Ref Spain, Ref U.S. Institute, EM1 and EM2.

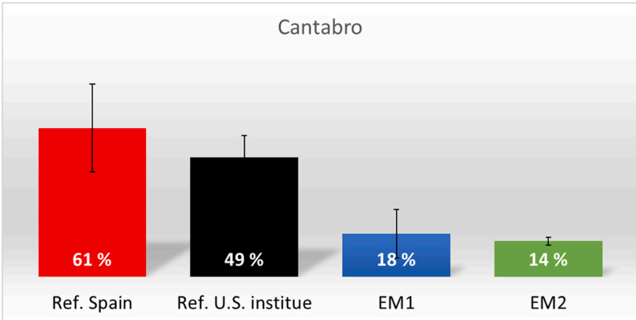

Fig. 17. Cantabro test results.

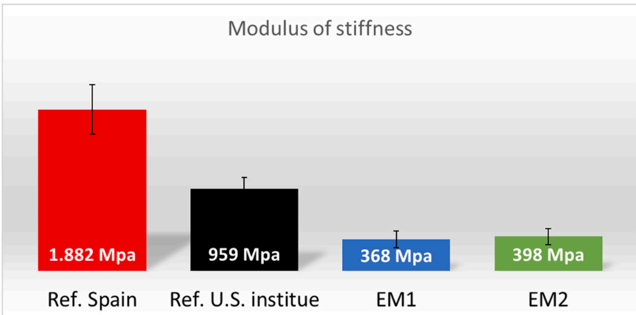

Fig. 18. Modulus of stiffness test results.

Taking into consideration the mechanical performance of the mixtures, the use of the induction protocol as method to cure the cold asphalt mixtures seems to see a feasible option, as it presents a proper mechanical behaviour decreasing the curing time. Concerning the application of the by-product instead of the virgin steel, it turns out to be a viable option, or even better, since it is a recycled material that allows the same reduction in curing time and presents a very similar mechanical performance.

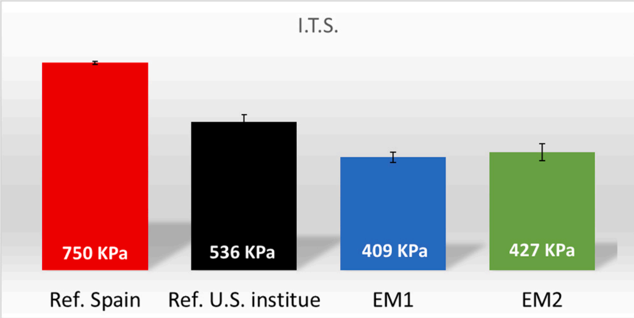

Fig. 19. I.T.S. test results.

Table 8
p-Values of the mechanical tests.

p-value	Cantabro	Indirect tensile strength	Stiffness
Ref. Spain – Ref. U.S.	0.394	0.000	0.004
Ref. Spain – EM1	0.044	0.000	0.002
Ref. Spain – EM2	0.047	0.000	0.030
Ref. U.S. – EM1	0.003	0.000	0.001
Ref. U.S. – EM2	0.001	0.003	0.030
EM1 – EM2	0.587	0.354	0.665

5. Conclusion

The feasibility of decreasing the curing time by applying induction heating and the impact of this on the rheological and mechanical capacity of cold asphalt mixtures have been evaluated. Two oven-cured mixtures were taken as reference and compared with two experimental cured by magnetic induction mixtures (one included magnetic by-products and another virgin steel fibers). The following conclusions were drawn:

- Magnetic induction as method to accelerate the curing is feasible, since it achieves the evaporation of 95% of the total water in the cold mix asphalt mixtures in only 2 h.
- The magnetically induction-cured mixtures, both with virgin steel fibers and by-products, showed lower bitumen aging than the oven-cured mix. This significantly reduced particle loss in the experimental mixtures. They also showed lower indirect tensile strength and stiffness.
- The use of industrial by-products is a viable option to replace virgin steel fibers in magnetic induction technology, since the curing time is the same and its rheological and mechanical properties are not compromised, even showing a better performance.

Considering that magnetic induction decreases the curing time, reduces the short aging and obtains a proper mechanical behaviour, future work will be carried out to scale this new fast curing process and evaluate other possible uses of induction magnetic technology in cold asphalt mixtures. The environmental and economic impact of this new process will determine its viability.

Declaration of Competing Interest

The authors declare that they have no known competing financial interests or personal relationships that could have appeared to influence the work reported in this paper.

Data Availability

Data will be made available on request.

Acknowledgements

This publication is part of the project SICA +(Ref. PDC2021-120824-I00), financed by MCIN/AEI/10.13039/501100011033 and by the European Union Next Generation EU/PRTR. The authors acknowledge and thank these institutions. The authors would like to thank Vicente Pérez Mena and María Del Mar Colás of Cepsa Comercial Petróleo S.A. for their collaboration. At the same time, we thank Paula Del Rio Gandarillas and Javier Menocal Allende, whose excellent work in the laboratory gave a fundamental added- value to the development of this research.

References

[1] S.S. Dash, A.K. Chandrappa, U.C. Sahoo, Design and performance of cold mix asphalt – A review, Constr. Build. Mater. vol. 315 (. 2022), https://doi.org/10.1016/j.conbuildmat.2021.125687.
[2] J. Chehovits and L. Galehouse, 2022. Energy usage and greenhouse gas emissions of pavement preservation processes for asphalt concrete pavements, in First International Conference on Pavement Preservation, 2010, pp. 27–42. Accessed: Aug. 09, 2022. [Online]. Available: https://trid.trb.org/view.aspx?id=919015.
[3] S. Jain, B. Singh, Cold mix asphalt: an overview, J. Clean. Prod. vol. 280 (2021), 124378, https://doi.org/10.1016/j.jclepro.2020.124378.
[4] P.T. Dorchies, 2008.The environmental road of the future: Analysis of energy consumption and greenhouse gas emissions, 2008. Accessed: Aug. 12, 2022. [Online]. Available: https://trid.trb.org/view/877014.
[5] S. Goyer, M. Dauvergne, L. Wendling, J. Fabre, C.D. La Roche, and V. Gaudefroy, Environmental evaluation of gravel emulsion Int. Symp. Life Cycle Assess. Constr., no. 2, pp. 170–178, 2012, [Online]. Available: https://hal.archives-ouvertes.fr/hal-00851066/.
[6] T. Saadoon, A. Garcia, B. Gómez-Meijide, Dynamics of water evaporation in cold asphalt mixtures, Mater. Des. vol. 134 (2017) 196–206, https://doi.org/10.1016/j.matdes.2017.08.040.
[7] Z. Zhao, J. Jiang, Z. Chen, F. Ni, Moisture migration of bitumen emulsion-based cold in-place recycling pavement after compaction: real-time field measurement and laboratory investigation, J. Clean. Prod. vol. 360 (2022), 132213, https://doi.org/10.1016/j.jclepro.2022.132213.
[8] A. Graziani, C. Godenzoni, F. Cardone, M. Bocci, Effect of curing on the physical and mechanical properties of cold-recycled bituminous mixtures, Mater. Des. vol. 95 (2016) 358–369, https://doi.org/10.1016/j.matdes.2016.01.094.
[9] X. Fang, A. Garcia-hernandez, P. Lura, Overview on cold cement bitumen emulsion asphalt, RILEM Tech. Lett. vol. 1 (2016) 116–121, https://doi.org/10.21809/rilemtechlett.2016.23.
[10] EAPA, "EAPA Asphalt in Figures 2017," Brussels, 2019. Accessed: Aug. 10, 2022. [Online]. Available: https://eapa.org/asphalt-in-figures-2017-view.
[11] I. Pérez, B. Gómez-Meijide, A.R. Pasandín, A. García, G. Airey, Enhancement of curing properties of cold in-place recycling asphalt mixtures by induction heating, Int. J. Pavement Eng. vol. 22 (3) (2021) 355–368, https://doi.org/10.1080/10298436.2019.1609674.
[12] P. Lastra-González, I. Indacoechea-Vega, M.A. Calzada-Pérez, D. Castro-Fresno, A. Vega-Zamanillo, Mechanical assessment of the induction heating as a method to accelerate the drying process of cold porous asphalt mixtures, Constr. Build. Mater. vol. 208 (2019) 646–650, https://doi.org/10.1016/j.conbuildmat.2019.03.053.
[13] K. Liu, C. Fu, P. Xu, S. Li, M. Huang, An eco-friendliness inductive asphalt mixture comprising waste steel shavings and waste ferrites, J. Clean. Prod. vol. 283 (2021), 124639, https://doi.org/10.1016/j.jclepro.2020.124639.
[14] World Steel Association, 2021. Climate Change and the Production of Iron and Steel: an Industry View, Brussels, Belgium., 2021. Accessed: Sep. 07, 2022. [Online]. Available: https://worldsteel.org/publications/policy-papers/climate-change-policy-paper/.
[15] Ateb, 2005. Pliego de mezclas bituminosas abiertas en frío, 2005. [Online]. Available: chrome-extension://efaidnbmnnnibpcajpcglclefindmkaj/http://ateb.es/images/pdf/PLI_MEZCLAS.pdf.
[16] Asphalt Institute, 1997. Institute Manual Series No.19, Third edition. 1997. doi: (AI MS 19).
[17] Á. García, E. Schlangen, M. Van De Ven, Q. Liu, A simple model to define induction heating in asphalt mastic (Jun.), Constr. Build. Mater. vol. 31 (2012) 38–46, https://doi.org/10.1016/J.CONBUILDMAT.2011.12.046.
[18] P.A. Tipler and G. Mosca, 2022. Física para la ciencia y la tecnología. Volumen 2A, Electricidad y magnetismo. 2020. Accessed: Aug. 19, 2022. [Online]. Available: https://buscador.bibliotecas.uc.cl/discovery/search?query=any,contains,tipler and mosca&tab=TODO&search_scope=TODO&vid=56PUC_INST:56PUC_INST&lang=es&offset=0.
[19] Q. Liu, W. Yu, S. Wu, E. Schlangen, P. Pan, A comparative study of the induction healing behaviors of hot and warm mix asphalt, Constr. Build. Mater. vol. 144 (2017) 663–670, https://doi.org/10.1016/j.conbuildmat.2017.03.195.
[20] C. Fu, K. Liu, P. Liu, M. Oeser, Experimental and numerical investigation of magnetic converge effect of magnetically conductive asphalt mixture, Constr. Build. Mater. vol. 360 (2022), 129626, https://doi.org/10.1016/j.conbuildmat.2022.129626.
[21] H. Xu, et al., Research on gradient characteristics and its prediction method of induction heating asphalt concrete, Constr. Build. Mater. vol. 309 (2021), 124920, https://doi.org/10.1016/j.conbuildmat.2021.124920.
[22] K. Liu, et al., Induction heating performance of asphalt pavements incorporating electrically conductive and magnetically absorbing layers, Constr. Build. Mater. vol. 229 (2019), 116805, https://doi.org/10.1016/j.conbuildmat.2019.116805.
[23] C. Fu, F. Wang, K. Liu, Q. Liu, P. Liu, M. Oeser, Inductive asphalt pavement layers for improving electromagnetic heating performance, Int. J. Pavement Eng. vol. 24 (1) (2023), https://doi.org/10.1080/10298436.2022.2159401.
[24] A. Graziani, A. Grilli, C. Mignini, A. Balzi, Assessing the field curing behavior of cold recycled asphalt mixtures, Adv. Mater. Sci. Eng. vol. 2022 (2022), https://doi.org/10.1155/2022/4157090.
[25] F. Barraj, A. Elkordi, Investigating the effect of using unclassified fractionated reclaimed asphalt pavement materials on the properties of hot mix asphalt, Constr. Build. Mater. vol. 353 (2022), 129099, https://doi.org/10.1016/j.conbuildmat.2022.129099.
[26] P. Lastra-gonzález, M.Á. Calzada-pérez, D. Castro-fresno, Á. Vega-zamanillo, I. Indacoechea-vega, Porous asphalt mixture with alternative aggregates and crumb-rubber modified binder at reduced temperature vol. 150 (2017) 260–267, https://doi.org/10.1016/j.conbuildmat.2017.06.008.
[27] A.H.A. Alhaddad, 2015. Construction of a Complex Shear Modulus Master Curve for Iraqi Asphalt Binder Using a Modified Sigmoidal Fitting, Int. J. Sci. Eng. Technol. Res., vol. Vol.04,Iss, no. July, pp. 0682–0690, 2015, doi: ISSN 2319–8885.
[28] A.A. Hatoum, J.M. Khatib, F. Barraj, A. Elkordi, Survival analysis for asphalt pavement performance and assessment of various factors affecting fatigue cracking based on LTPP data, Sustain vol. 14 (19) (2022), https://doi.org/10.3390/su141912408.